Plenary Paper

blood

VASCULAR BIOLOGY

ADAMTS13 controls vascular remodeling by modifying VWF reactivity during stroke recovery

Haochen Xu,* Yongliang Cao,* Xing Yang,* Ping Cai, Lijing Kang, Ximin Zhu, Haiyu Luo, Lu Lu, Lixiang Wei, Xiaofei Bai, Yuanbo Zhu, Bing-Qiao Zhao, and Wenying Fan

State Key Laboratory of Medical Neurobiology, Institutes of Brain Science, Collaborative Innovation Center for Brain Science and School of Basic Medical Sciences, Fudan University, Shanghai, China

Key Points

- ADAMTS13 controls key steps of vascular remodeling during stroke recovery.
- Recombinant ADAMTS13 enhances ischemic neovascularization and vascular repair.

Angiogenic response is essential for ischemic brain repair. The von Willebrand factor (VWF)–cleaving protease disintegrin and metalloprotease with thrombospondin type I motif, member 13 (ADAMTS13) is required for endothelial tube formation in vitro, but there is currently no in vivo evidence supporting a function of ADAMTS13 in angiogenesis. Here we show that mice deficient in ADAMTS13 exhibited reduced neovascularization, brain capillary perfusion, pericyte and smooth muscle cell coverage on microvessels, expression of the tight junction and basement membrane proteins, and accelerated blood-brain barrier (BBB) breakdown and extravascular deposits of serum proteins in the peri-infarct cortex at 14 days after stroke. Deficiency of VWF or anti-VWF antibody treatment significantly increased microvessels, perfused capillary length, and reversed pericyte loss and BBB changes in *Adamts13*$^{-/-}$ mice. Furthermore, we observed that ADAMTS13 deficiency decreased angiopoietin-2 and galectin-3 levels in the isolated brain microvessels, whereas VWF deficiency had the opposite effect. Correlating with this, overexpression of angiopoietin-2 by adenoviruses treatment or administration of recombinant galectin-3 normalized microvascular reductions, pericyte loss, and BBB breakdown in *Adamts13*$^{-/-}$ mice. The vascular changes induced by angiopoietin-2 overexpression and recombinant galectin-3 treatment in *Adamts13*$^{-/-}$ mice were abolished by the vascular endothelial growth factor receptor-2 antagonist SU1498. Importantly, treating wild-type mice with recombinant ADAMTS13 at 7 days after stroke markedly increased neovascularization and vascular repair and improved functional recovery at 14 days. Our results suggest that ADAMTS13 controls key steps of ischemic vascular remodeling and that recombinant ADAMTS13 is a putative therapeutic avenue for promoting stroke recovery. (*Blood*. 2017;130(1):11-22)

Introduction

Stroke is a leading cause of long-term disability worldwide; however, there are no effective therapies available for promoting stroke recovery. Brain ischemia stimulates ongoing neurogenesis, which leads neuronal precursor cells to migrate to ischemic regions to support remodeling of damaged tissue.[1] Despite multiple reports that indicate stem cell therapy holds promise in enhancing functional restoration in stroke, it has been limited by poor survival and differentiation of transplanted cells.[2,3] Studies have shown that brain ischemia also induces vascular remodeling in the peri-infarct area.[4,5] Angiogenic vessels secrete neurotrophic factors and chemokines, which may create a suitable microenvironment within the damaged brain that supports the survival of newly formed neurons.[6] In stroke patients, increased vascularization in the peri-infarct area is correlated with longer survival, indicating that the angiogenic response after stroke is important for neurological recovery.[7] Hence, understanding the mechanisms underlying angiogenesis and vascular repair after brain injury may have important therapeutic value for stroke and degenerative diseases.

von Willebrand factor (VWF) is a large multimeric glycoprotein that plays an important role in hemostasis, thrombus formation, and inflammatory cell recruitment.[8] VWF is normally synthesized by vascular endothelial cells and megakaryocytes and stored in Weibel-Palade bodies of endothelial cells and platelet α-granules.[9] During vascular injury, VWF is secreted as hyperactive ultralarge multimers (UL-VWFs), which are rapidly cleaved by a disintegrin and metalloprotease with thrombospondin type I motif, member 13 (ADAMTS13) into smaller, less reactive fragments.[10] Deficiency of ADAMTS13 activity results in accumulation of UL-VWF in circulation and causes thrombotic thrombocytopenic purpura.[10] In addition, ADAMTS13 was also shown to reduce both thrombosis and inflammation through the cleavage of VWF.[11-13]

Angiogenesis is a complex process constituting multiple steps. Vascular endothelial growth factor (VEGF) and VEGF receptor 2 (VEGFR-2) initiate angiogenesis, and angiopoietins (Angs) 1 and 2 are implicated in vascular maturation and stabilization.[14] In angiogenic tissues, Ang-2 was shown to act synergistically with VEGF-A to

Submitted 20 October 2016; accepted 16 April 2017. Prepublished online as *Blood* First Edition paper, 20 April 2017; DOI 10.1182/blood-2016-10-747089.

*H.X., Y.C., and X.Y. contributed equally to this study.

The online version of this article contains a data supplement.

There is an Inside *Blood* Commentary on this article in this issue.

The publication costs of this article were defrayed in part by page charge payment. Therefore, and solely to indicate this fact, this article is hereby marked "advertisement" in accordance with 18 USC section 1734.

increase angiogenesis.[15] VWF is the main constituent protein of endothelial Weibel-Palade bodies, which also contain Ang-2 and other angiogenesis mediators.[16,17] Loss of VWF resulted in increased release of Ang-2 and activation of VEGFR-2 and promoted VEGFR-2–dependent angiogenesis.[18] Furthermore, when the phosphorylation of VEGFR-2 was inhibited, the increased in vitro angiogenesis in VWF-deficient cells was normalized.[18] However, other VWF-associated angiogenic regulators may also be involved in the antiangiogenic effects of VWF. In particular, galectin-3 (Gal-3) is able to directly bind to VWF and can induce phosphorylation of VEGFR-2.[19,20] Recent studies suggest that VWF participates in multiple vascular processes. The importance of VWF in vessel patterning has been reported, and the role of VWF in vascular smooth muscle cell coverage during vascular development was demonstrated[18,21] Because ADAMTS13 proteolytically degrades VWF,[10] it may also play a role in angiogenesis. Indeed, ADAMTS13 was recently reported to increase VEGFR-2 phosphorylation and promote proliferation and migration of human umbilical vein endothelial cells in vitro.[22] However, whether ADAMTS13 plays a role in vascular regeneration in vivo remains elusive.

In this study using the *Adamts13*$^{-/-}$ and *Adamts13*$^{-/-}$*Vwf*$^{-/-}$ mice, we have investigated the mechanism by which the VWF-cleaving proteinase ADAMTS13 modulates neovascularization and blood-brain barrier (BBB) integrity in the ischemic brain and describe a new mechanism involving Ang-2, Gal-3, and phosphorylated VEGFR-2 (pVEGFR-2). We have also studied whether late administration of recombinant ADAMTS13 (rADAMTS13) enhances vascular repair and regeneration of blood vessels damaged by stroke.

Methods

Animals

The *Adamts13*$^{-/-}$ and *Vwf*$^{-/-}$ mice (The Jackson Laboratory) were crossed to generate *Adamts13*$^{-/-}$*Vwf*$^{-/-}$ mice, which were on C57BL/6 background. All experimental procedures were approved by the Animal Care and Use Committee of Institutes of Brain Science, Fudan University. Details can be seen in the supplemental Methods, available on the *Blood* Web site.

Distal middle cerebral artery occlusion

Cortical cerebral ischemia were produced by electrocoagulation of the distal portion of the right middle cerebral artery, as described elsewhere (supplemental Methods).[23]

Treatment regimens

Recombinant human ADAMTS13 (rADAMTS13; 25 ng in 2 μL phosphate-buffered saline [PBS]; R&D Systems) was injected either into the lateral ventricle (25 ng in 2 μL PBS) or IV (50 μg/kg) into mice once a day for 1 week.[13,24] Treatment with rADAMTS13 effectively induced the expression of human ADAMTS13 at 14 days after stroke (supplemental Figure 6A). To examine the effects of a combined rADAMTS13 and VWF approach on neovascularization and BBB permeability, human VWF (5 μg/mouse; Haematologic Technologies, Essex Junction, VT) was administrated IV with rADAMTS13 into mice once per day for 1 week.[25] Because the half-life of human VWF is very short in mice,[26,27] daily administration was performed. VEGFR-2 antagonist Su1498 (250 ng in 2 μL PBS containing 1% dimethyl sulfoxide; Abcam, Cambridge, MA), recombinant human galectin-3 (rGal-3; 5 μg/mouse; Peprotech, Rocky Hill, NJ) or rabbit anti-VWF antibody (6 μg/g body weight; Dako, Carpinteria, CA) was administered for 1 week.[28,29] Angiopoietin-2 adenovirus or control only expressing red fluorescent protein was injected into the right striatum (1 μL of 1.2×10^{13} viral genomes/mL). All treatments were started at 7 days after cerebral ischemia (supplemental Methods).

In vivo multiphoton microscopy analysis

In vivo time-lapse images were taken using a multiphoton laser-scanning microscope (FV1200MPE, Olympus, Japan). For determination of the perfused microvascular length, fluorescein isothiocyanate (FITC)-conjugated dextran (FITC-dextran; molecular weight [MW] = 2 000 000 Da, Sigma-Aldrich; 0.1 mL of 10 mg/mL) was injected IV. For determination of cortical cerebrovascular permeability, FITC-dextran (MW = 40 000 Da, Sigma-Aldrich; 0.1 mL of 10 mg/mL) was injected IV and multiphoton time-lapse imaging was taken (supplemental Methods).

Statistical analysis

Data are represented as mean ± standard deviation (SD) and were analyzed using 1-way analysis of variance (ANOVA) followed by the Bonferroni multiple comparison test. When 2 groups were compared, unpaired 2-tailed Student *t* test was used. Differences were considered significant with a $P < .05$.

Results

ADAMTS13 deficiency reduces neovascularization during stroke recovery

To address the role of ADAMTS13 on neovessel formation during stroke recovery, we used *Adamts13*$^{-/-}$ mice. No significant differences were observed in brain microvascular structure (microvascular length/area and the length of perfused cortical microvessels) and permeability of the BBB between wild-type (WT) and *Adamts13*$^{-/-}$ mice after sham operation (Figures 1B,E and 2A). We subjected mice to distal middle cerebral artery obstruction, and analyzed the blood vessels in the peri-infarct cortical areas. Hematoxylin and eosin staining of coronal section shows the areas surrounding the infarct (peri-infarct cortical areas) used for all histological measurements and in vivo multiphoton microscopy analysis (Figure 1A). At 14 days after stroke, *Adamts13*$^{-/-}$ mice showed significant reductions in both microvascular length and area, by 30% and 47% (Figure 1B), respectively, compared with WT mice. There was also a significant decrease in microvascular length and area in *Adamts13*$^{-/-}$ mice subjected to stroke compared with sham-operated mice. Moreover, vascular branches and the number of positive isolectinB4 (IB4^{+}) endothelial tip cells were decreased by 44% and 59%, respectively, in *Adamts13*$^{-/-}$ mice (Figure 1C; supplemental Figure 1). We further examined the effect of ADAMTS13 deficiency on endothelial proliferation by repeated 5-bromo-2′-deoxyuridine (BrdU) administration and found that the numbers of BrdU^{+}/CD31^{+} endothelial cells were decreased by 47% in *Adamts13*$^{-/-}$ mice compared with WT mice (Figure 1D). These data suggest that ADAMTS13 has a modulatory role in neovessel formation by regulating vessel sprouting and endothelial proliferation.

Based on the vascular data obtained by histological quantification, we assessed cerebrovascular perfusion using in vivo multiphoton microscopy imaging of IV injected FITC-dextran (MW = 2 000 000 Da). This analysis indicated a 63% reduction in the length of perfused cortical microvessels in *Adamts13*$^{-/-}$ mice compared with WT mice (Figure 1E). Next, we evaluated the functionality of cortical vessels by in vivo administration of tomato-lectin. The area of tomato-lectin–perfused vessels was profoundly reduced by 37% in *Adamts13*$^{-/-}$ mice (Figure 1F). Thus, ADAMTS13 deficiency leads to significant reductions in vascularization and brain vascular perfusion after stroke.

ADAMTS13 deficiency disrupts vascular integrity and exacerbates BBB breakdown

Cerebrovascular integrity, which is critical for proper vascular function, is disrupted after stroke and can last up to several weeks.[30,31] To

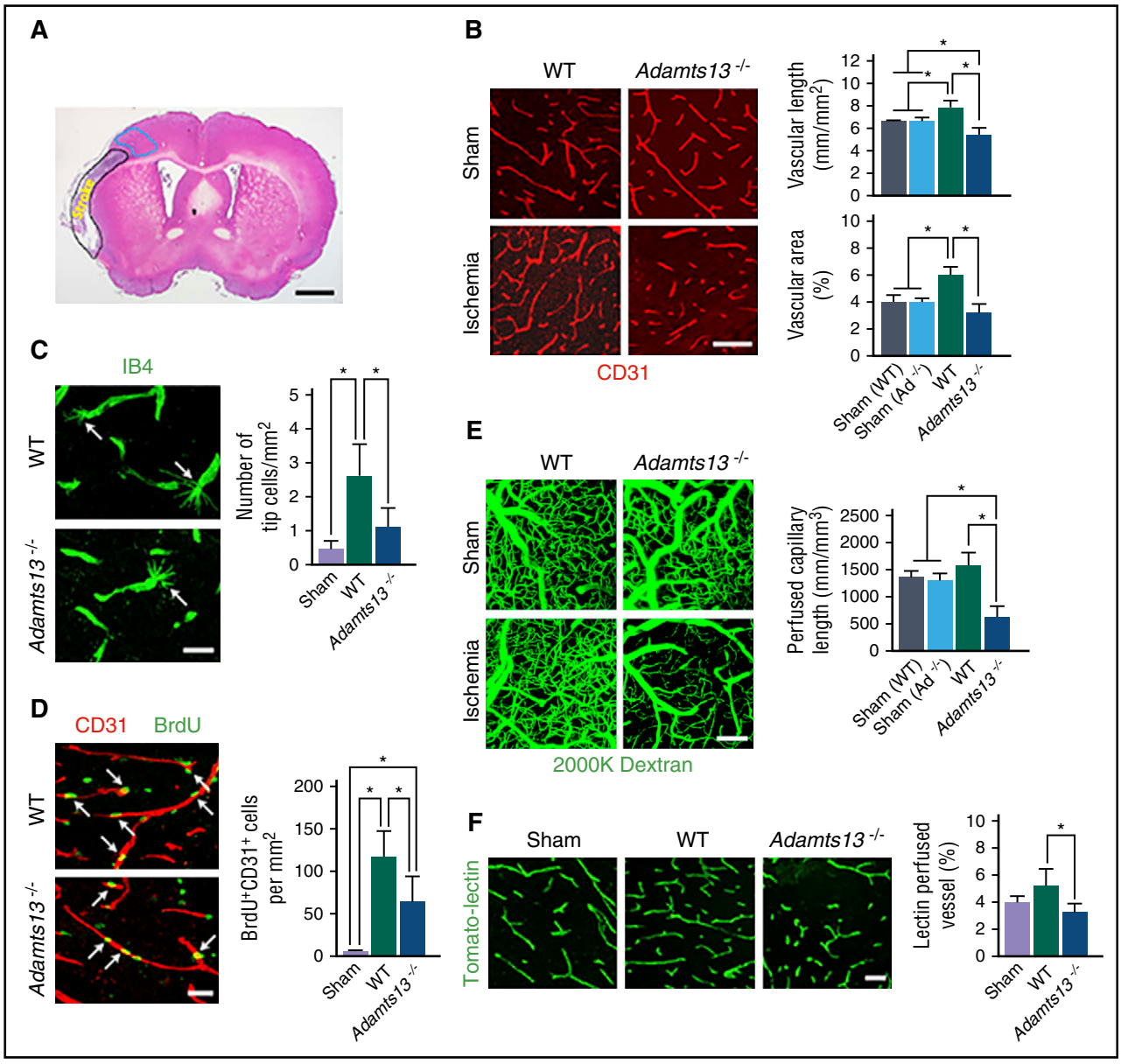

Figure 1. ADAMTS13 deficiency reduces neovascularization during the recovery phase after stroke. (A) Hematoxylin and eosin–stained coronal sections of ischemic brain at 14 days after stroke. The broken blue line shows the location used for all histological measurements and in vivo multiphoton microscopy analysis in the peri-infarct cortical areas (the areas surrounding the infarct). Scale bar = 1 mm. (B) Representative images of $CD31^+$ microvessels at 14 days after stroke or sham operation in WT and *Adamts13*$^{-/-}$ mice, and quantification of $CD31^+$ microvascular length and percent area occupied by vascular structures for each group. Scale bar = 100 μm. (C-D) Representative images of vascular branches, $IB4^+$ endothelial tip cells and $BrdU^+/CD31^+$ endothelial cells in WT and *Adamts13*$^{-/-}$ mice subjected to ischemia, and quantification of the data in WT and *Adamts13*$^{-/-}$ mice subjected to ischemia or sham operation. Bar = 20 μm. (E) Representative in vivo multiphoton microscopic images of cortical capillaries in real time in the living mouse brain. For visualization of the brain vasculature, FITC-dextran (MW = 2 000 000 Da) was injected IV just before beginning the imaging experiment. (Right) Quantification of perfused capillary length in WT and *Adamts13*$^{-/-}$ mice subjected to ischemia or sham operation. $Ad^{-/-}$, *Adamts13*$^{-/-}$. Bar = 100 μm. (F) Representative images of tomato-lectin–perfused vessels and quantification of lectin-perfused vessel area in WT and *Adamts13*$^{-/-}$ mice subjected to ischemia or sham operation. Scale bar = 50 μm. Values are mean ± SD. One-way ANOVA followed by the Bonferroni multiple comparison test. n = 6 per group, $*P < .05$.

investigate the role of ADAMTS13 on cerebrovascular permeability, we performed in vivo time-lapse multiphoton imaging assays after intravenous administration of a vascular tracer, FITC-dextran (MW = 40 000 Da). The results revealed that high-molecular-weight FITC-dextran did not leak in cortical vasculature in the sham group (Figure 2A). As described previously, we found significant increase in neovascularization in the peri-infarct cortical areas at 14 days after stroke compared with sham-operated brains (Figure 1B-D; supplemental Figure 1). However, immunostaining for plasma-derived immunoglobulin G (IgG) and endothelial cells revealed significant perivascular IgG accumulation in these peri-infarct areas (Figure 2B). Moreover, we found that the microvessel wall in the peri-infarct areas showed serious leakage of the FITC-dextran propagating to the nearby parenchyma (Figure 2A), where new vessels are located (Figures 1B-D and 2B), indicating that newly formed vessels are permeable and not yet fully developed. Quantitative analysis demonstrated that BBB permeability was greatly increased by 82% in *Adamts13*$^{-/-}$ mice compared with WT controls (Figure 2A). Consistent with these findings, *Adamts13*$^{-/-}$ mice exhibited a significant increase in dextran leakage where dextran was injected IV (Figure 2C), showing a

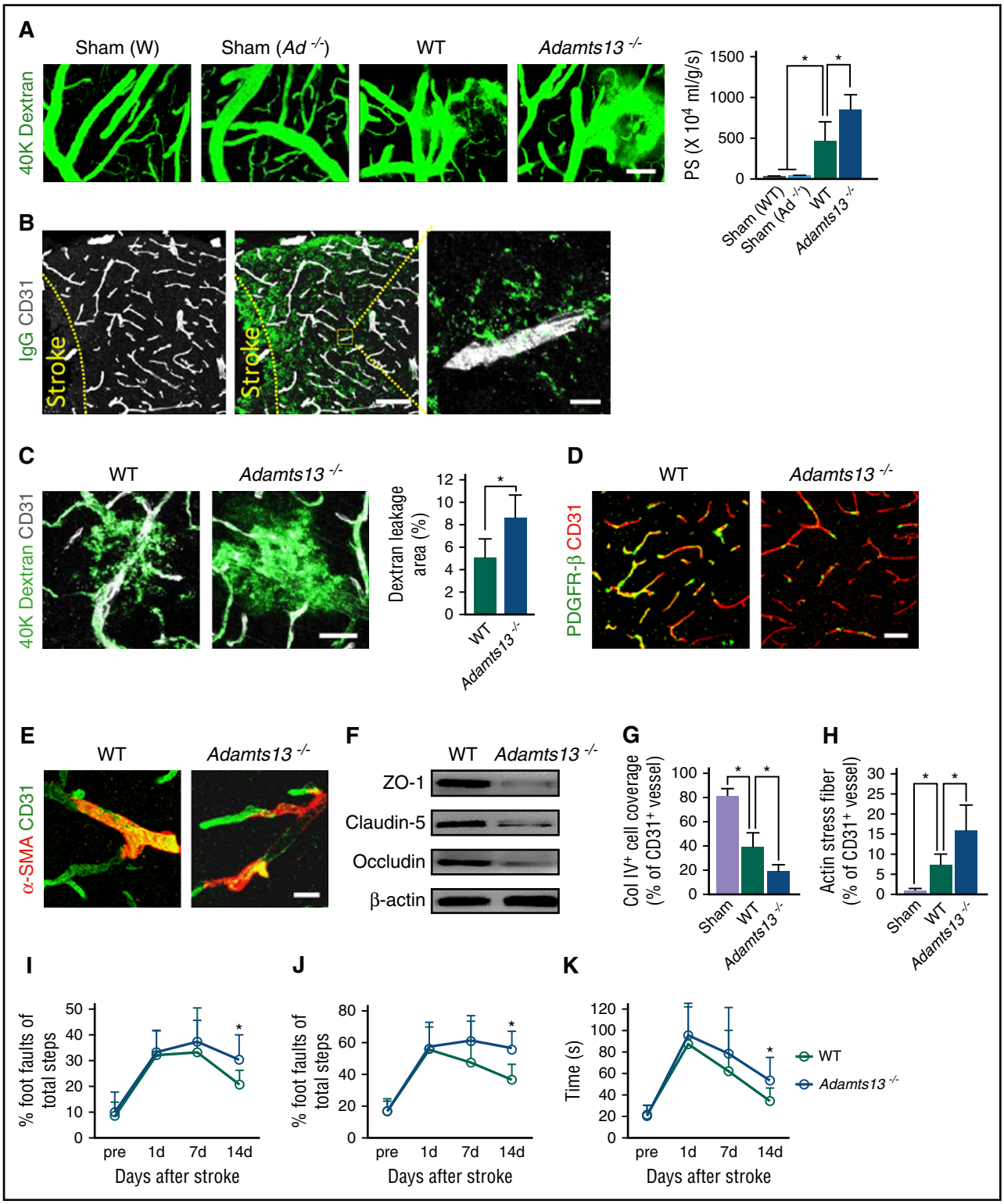

Figure 2. Increased BBB breakdown and loss of the BBB properties in ADAMTS13-deficient mice. (A) Representative in vivo multiphoton microscopic images (left) of IV injected FITC-dextran (MW = 40 000 Da) leakage from cortical vessels and quantification of the permeability surface (PS) product (right) of FITC-dextran in WT and *Adamts13*$^{-/-}$ mice subjected to ischemia or sham operation. Ad$^{-/-}$, *Adamts13*$^{-/-}$. Scale bar = 50 μm. Values are mean ± SD. One-way ANOVA followed by Bonferroni's multiple comparison test. n = 6 per group, *$P < .05$. (B) Representative images of IgG deposits (green) and CD31^{+} (white) in the peri-infarct cortical areas 14 days after stroke in WT mice. (Right) Higher magnification of the box in the center panel. Scale bar = 100 μm and 10 μm (right). (C) (Left) At 14 days after stroke, mice were given an intravascular injection of 40 000 Da FITC-labeled dextran, and brain sections were stained with CD31. (Right) Quantification of extravascular dextran fluorescence in WT and *Adamts13*$^{-/-}$ mice subjected to stroke. Scale bar = 30 μm. Values are mean ± SD. Unpaired 2-tailed Student *t* test. n = 6 per group, *$P < .05$. (D-E) Representative images of PDGFR-β^{+} pericyte and α-SMA^{+} smooth muscle cell coverage on CD31^{+} microvessels in WT and *Adamts13*$^{-/-}$ mice subjected to stroke. Scale bar = 50 μm (D) and 10 μm (E). (F) Immunoblots showing ZO-1, occludin, and claudin 5 levels in brain microvessels of WT and *Adamts13*$^{-/-}$ mice subjected to stroke. (G) Quantification of collagen IV^{+} (Col IV) basement membrane coverage on CD31^{+} microvessels in WT and *Adamts13*$^{-/-}$ mice subjected to ischemia or sham operation. Values are mean ± SD. One-way ANOVA followed by Bonferroni multiple comparison test. n = 6 per group, *$P < .05$. (H) Quantification of actin stress fiber formation on CD31^{+} microvessels in WT and *Adamts13*$^{-/-}$ mice subjected to ischemia or sham operation. Values are mean ± SD. One-way ANOVA followed by Bonferroni multiple comparison test. n = 6 per group, *$P < .05$. (I-K) Beam-walking and tape removal tests in WT and *Adamts13*$^{-/-}$ mice. Values are mean ± SD. Unpaired, 2-tailed Student *t* test. n = 8 per group, *$P < .05$. d, day.

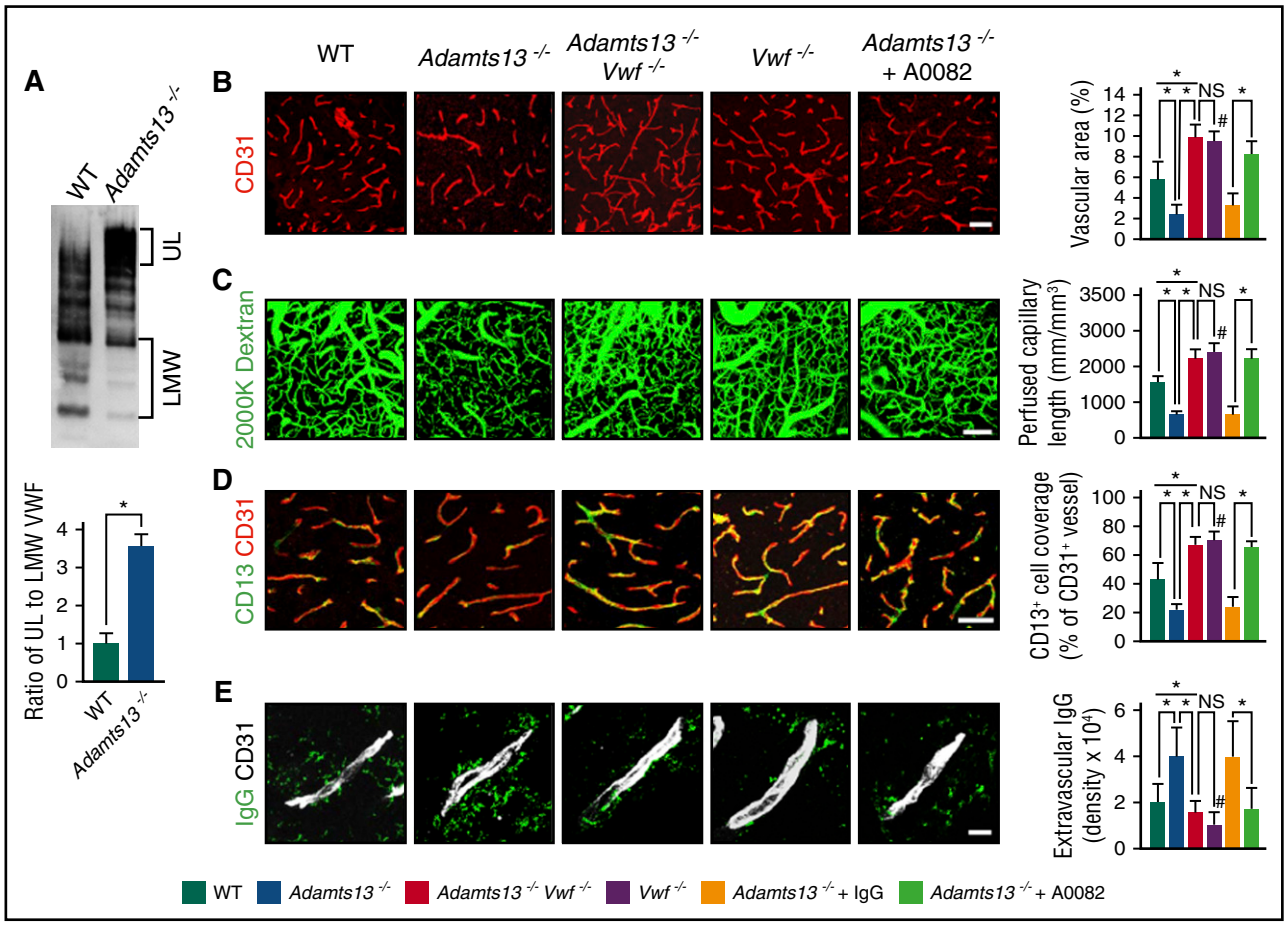

Figure 3. VWF deficiency and neutralization of VWF in *Adamts13*$^{-/-}$ mice enhance neovascularization and decrease vascular damage. (A) Plasma VWF multimers from WT and *Adamts13*$^{-/-}$ mice were determined using agarose gel electrophoresis and western blotting. (Bottom) Quantitative analysis of the ratio of ultralarge (UL) to low-molecular-weight (LMW) VWF multimers in each group. Values are mean ± SD. Unpaired, 2-tailed Student *t* test. n = 4 per group, **P* < .05. (B) Representative images of CD31$^+$ microvessels at 14 days after stroke in WT, *Adamts13*$^{-/-}$, *Adamts13*$^{-/-}$ *Vwf*$^{-/-}$, *Vwf*$^{-/-}$ mice, and *Adamts13*$^{-/-}$ mice treated with the anti-VWF antibody, and quantification of percent area occupied by vascular structures for each group. (C) Representative images of multiphoton microscopy of IV injected FITC-dextran (MW = 2 000 000 Da) at 14 days after stroke in WT, *Adamts13*$^{-/-}$, *Adamts13*$^{-/-}$ *Vwf*$^{-/-}$, *Vwf*$^{-/-}$ mice, and *Adamts13*$^{-/-}$ mice treated with the anti-VWF antibody, and quantification of perfused capillary length for each group. (D) Representative images and quantification of CD13$^+$ pericyte coverage on CD31$^+$ microvessels at 14 days after stroke in WT, *Adamts13*$^{-/-}$, *Adamts13*$^{-/-}$ *Vwf*$^{-/-}$, *Vwf*$^{-/-}$ mice, and *Adamts13*$^{-/-}$ mice treated with the anti-VWF antibody. (E) Representative images of IgG deposits and CD31$^+$ microvessels at 14 days after stroke in WT, *Adamts13*$^{-/-}$, *Adamts13*$^{-/-}$ *Vwf*$^{-/-}$, *Vwf*$^{-/-}$ mice, and *Adamts13*$^{-/-}$ mice treated with the anti-VWF antibody, and quantification of extravascular IgG deposits for each group. Scale bars = 50 μm (B-D) and 10 μm (E). Values are mean ± SD. One-way ANOVA followed by Bonferroni multiple comparison test. n = 6 per group, **P* < .05, #*P* < .05 compared with WT. NS, not significant.

significant increase in BBB permeability. When the BBB is disrupted, endogenous macromolecules in circulation can accumulate in the brain parenchyma.[32,33] We then quantified the extravasation of circulating protein IgG in the brains of mice. Immunostaining of IgG with CD31 indicated a 2.3-fold greater extravascular accumulation of IgG in *Adamts13*$^{-/-}$ mice compared with WT controls (supplemental Figure 2A). Next, we compared vascular phenotype in *Adamts13*$^{-/-}$ mice with WT littermate and nonlittermate mice. At 14 days after stroke, *Adamts13*$^{-/-}$ mice showed significant reductions in both microvascular length and area compared with WT littermate and nonlittermate mice (supplemental Figure 3A). We also repeated the experiment to detect cerebrovascular perfusion using in vivo multiphoton microscopy imaging of IV injected FITC-dextran (MW = 2 000 000 Da). This analysis indicated ~60% reduction in perfused cortical microvascular length in *Adamts13*$^{-/-}$ mice compared with WT littermate and nonlittermate mice (supplemental Figure 3B). In addition, multiphoton microscopy of IV injected FITC-dextran (MW = 40 000 Da) revealed an increase in BBB permeability in *Adamts13*$^{-/-}$ mice compared with WT littermate and nonlittermate mice (supplemental Figure 3C). There was no significant difference in vascularization and vascular perfusion between littermate and nonlittermate WT mice.

Pericytes contribute to the maintenance of BBB integrity.[34] Using staining for pericyte markers platelet-derived growth factor receptor-β (PDGFR-β) and CD13,[33,34] we found that PDGFR-β$^+$ pericyte coverage was 52% less and CD13$^+$ pericyte coverage was 53% less in *Adamts13*$^{-/-}$ mice compared with WT mice (Figure 2D; supplemental Figure 2B-C). Smooth muscle marker α (α-SMA) was also strongly reduced in the surrounding vessels in *Adamts13*$^{-/-}$ mice (Figure 2E; supplemental Figure 2D). Together with these findings, the BBB tight junction proteins including ZO-1, occludin, and claudin 5 in brain microvessels were reduced (Figure 2F; supplemental Figure 2E-G), and collagen IV$^+$ basement membrane coverage was 54% less in *Adamts13*$^{-/-}$ mice (Figure 2G). In agreement with this result, actin stress fiber formation, which is associated with irregular endothelial junctions and elevated endothelial permeability,[35] was increased by 2.2-fold in *Adamts13*$^{-/-}$ mice (Figure 2H). In addition, *Adamts13*$^{-/-}$ mice had more severe neurological deficits as assayed by the beam-walking test and adhesive tape removal test (Figure 2I-K).

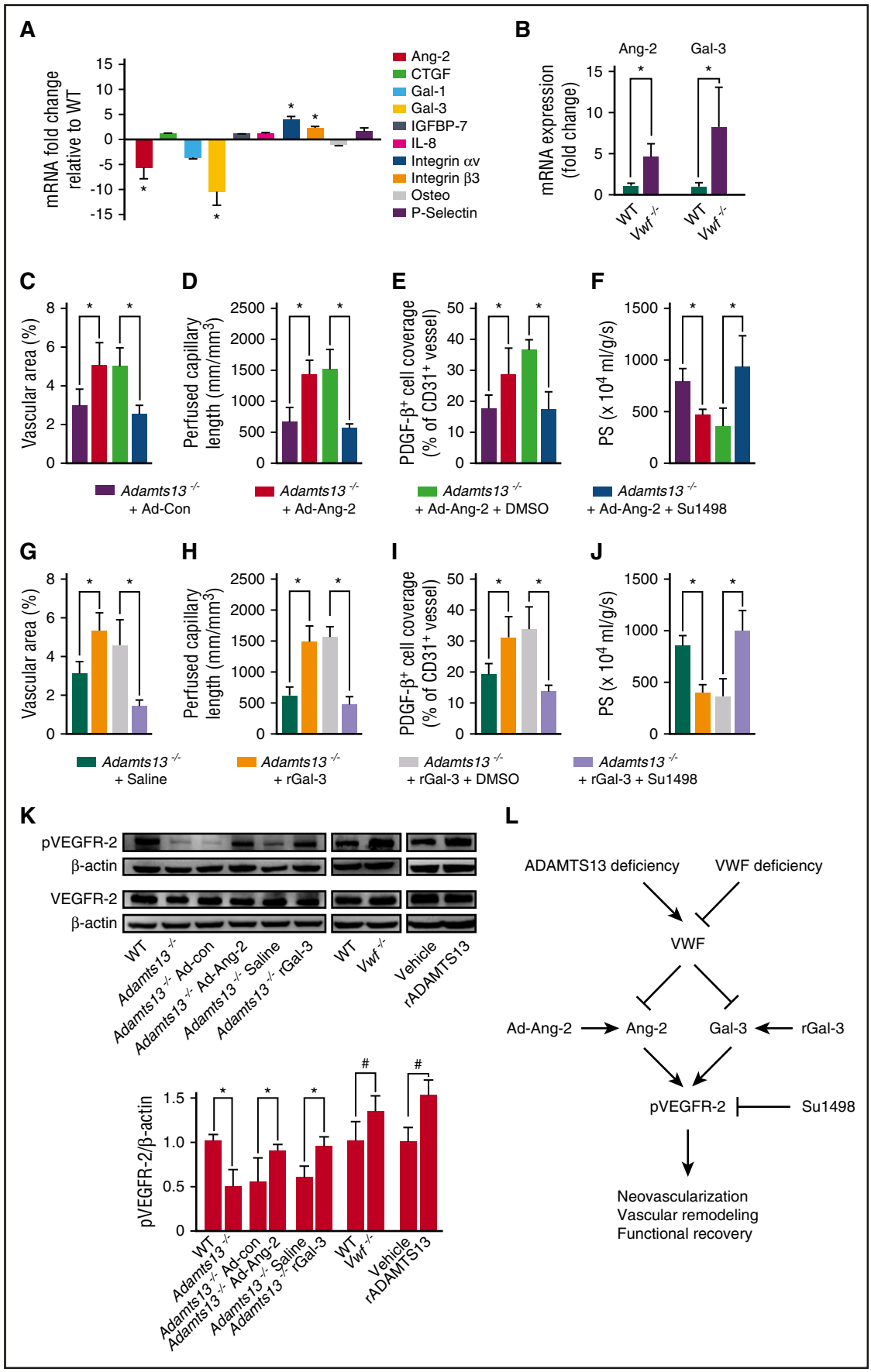

Figure 4.

ADAMTS13 regulates neovascularization and BBB permeability through VWF- Ang-2/Gal-3–dependent VEGFR-2 activation

To investigate the mechanism underlying ADAMTS13 deficiency-mediated microvascular reduction and BBB breakdown, we studied VWF, which is the only known substrate for ADAMTS13. Previous studies have shown that phenotypes in the *Adamts13*$^{-/-}$ mice, such as atherosclerosis and thrombosis, were linked to VWF.[11,12,36] Furthermore, the lack of VWF caused enhanced angiogenesis in the Matrigel plug assay and increased vascular density in the mouse ear.[18] In the present study, we observed that 14 days after stroke, the ratio of plasma UL-VWF to low-molecular-weight VWF multimers was significantly increased in *Adamts13*$^{-/-}$ mice compared with WT mice (Figure 3A). Therefore, we hypothesized that the reduced vascularization in ADAMTS13-deficient mice might be mediated through a VWF-dependent mechanism. We found that *Adamts13*$^{-/-}$*Vwf*$^{-/-}$ mice had marked increase in microvessels in the peri-infarct cortex compared with *Adamts13*$^{-/-}$ (Figure 3B). In vivo multiphoton microscopy indicated a significant 3.5-fold increase in the length of perfused cortical microvessels in *Adamts13*$^{-/-}$*Vwf*$^{-/-}$ mice compared with *Adamts13*$^{-/-}$ mice (Figure 3C). *Adamts13*$^{-/-}$*Vwf*$^{-/-}$ microvessels also showed significantly greater increase in CD13^{+} pericyte coverage compared with *Adamts13*$^{-/-}$ (Figure 3D). Furthermore, IgG perivascular accumulation was significantly reduced in *Adamts13*$^{-/-}$*Vwf*$^{-/-}$ mice compared with *Adamts13*$^{-/-}$ (Figure 3E), indicating a significant reduction in BBB permeability. The *Adamts13*$^{-/-}$*Vwf*$^{-/-}$ mice also exhibited significantly increased microvascular area, length of perfused cortical microvessels and CD13^{+} pericyte coverage, and reduced perivascular IgG deposits compared with WT mice. We then detected vascular phenotype in the brain of *Vwf*$^{-/-}$ mice after stroke. We found that *Vwf*$^{-/-}$ mice had dramatically increased microvessels, more perfused cortical microvessels and pericyte coverage, and reduced IgG perivascular accumulation compared with the WT mice (Figure 3B-E). No significant differences in the vascular phenotype were observed in mice deficient in both ADAMTS13 and VWF compared with mice deficient in VWF alone. Similarly, anti-VWF antibody treatment reversed the vascular phenotype in *Adamts13*$^{-/-}$ mice (Figure 3B-E). Together, these data suggest that the impaired vascular remodeling observed in *Adamts13*$^{-/-}$ mice is VWF-dependent.

Next, we used quantitative polymerase chain reaction (PCR) to assess the messenger RNA expression of 10 molecules potentially important for vascular integrity in brain microvessels isolated from ADAMTS13-deficient mutants and controls 10 days after stroke.[37] Of the 10 genes analyzed, Ang-2 and Gal-3 showed the largest alteration in gene expression, with more than 5.5-fold downregulation in *Adamts13*$^{-/-}$ mice (Figure 4A). In contrast, VWF deficiency resulted in a significant increase in Ang-2 and Gal-3 levels in the isolated brain microvessels (Figure 4B). Ang-2 is an antagonist of the vascular receptor tyrosine kinase Tie2 and is essential for angiogenesis and maintenance of endothelial integrity.[38,39] Gal-3 is a proangiogenic factor,[40] and genetic ablation of Gal-3 was shown previously to suppress angiogenesis after stroke.[41] We therefore hypothesized that endogenous ADAMTS13 may contribute to vascular remodeling during stroke recovery by regulating Ang-2 or Gal-3. To examine this hypothesis, we studied the effects of overexpression of Ang-2 by adenoviruses treatment, and of exogenous administration of rGal-3 in *Adamts13*$^{-/-}$ mice. Injection of Ang-2 adenovirus in *Adamts13*$^{-/-}$ mice increased microvascular area, perfused cortical microvascular length, and pericyte coverage by 72%, 123% and 64%, respectively, compared with control virus (Figure 4C-E; supplemental Figure 4A). Using multiphoton microscopy of IV injected FITC-dextran, we observed a significant reduction in BBB damage in *Adamts13*$^{-/-}$ mice treated with Ang-2 adenovirus (Figure 4F; supplemental Figure 4A). Also, administration of rGal-3 resulted in a significant increase in microvascular area, the length of perfused cortical microvascular and pericyte coverage, and a substantial reduction in BBB disruption in *Adamts13*$^{-/-}$ mice (Figure 4G-J; supplemental Figure 4B).

The peri-infarct areas upregulate angiogenic signaling after stroke through the proangiogenic receptor's VEGFR-2 activation.[42] Western blot analysis of the isolated brain microvessels revealed a significant reduction in the phosphorylation of VEGFR-2 at tyrosine 1059 in *Adamts13*$^{-/-}$ mice compared with WT mice (Figure 4K). In contrast, *Vwf*$^{-/-}$ mice exhibited significantly increased VEGFR-2 phosphorylation compared with WT mice. Neither *Adamts13*$^{-/-}$ nor *Vwf*$^{-/-}$ mice showed changes in VEGFR2 expression compared with WT mice (Figure 4K, top left]; supplemental Figure 2H). These results indicate that ADAMTS13 and VWF play opposite roles in regulating the phosphorylation of VEGFR-2 during stroke recovery. Consistent with findings that both Ang-2 and Gal-3 activate VEGFR-2 signaling,[20,43] we found that adenoviral-mediated overexpression of Ang-2 or treatment with rGal-3 reversed downregulation of phosphorylated VEGFR-2 in *Adamts13*$^{-/-}$ mice (Figure 4K). As expected, the VEGFR-2 antagonist SU1498 led to a significant decrease in microvascular area, which is the length of perfused cortical microvascular and pericyte coverage in *Adamts13*$^{-/-}$ mice treated with Ang-2 adenoviruses or rGal-3 (Figure 4C-E,G-I; supplemental Figure 4A-B); this was accompanied by increased BBB breakdown (Figure 4F,J; supplemental Figure 4A-B). Collectively, these data indicate that VEGFR-2 is a downstream molecule of Ang-2 and Gal-3 signaling.

rADAMTS13 increases neovascularization and improves vascular function and behavioral outcome during the delayed stages after stroke

Data described previously demonstrated that lack of ADAMTS13 reduced neovascularization and aggravated vascular defects after stroke.

Figure 4. ADAMTS13 regulates neovascularization and vascular permeability through the Ang-2/Gal-3–mediated VEGFR-2 phosphorylation. (A) Quantitative PCR was used in freshly isolated brain microvessels to evaluate the expression of molecules potentially important for vascular integrity in WT and *Adamts13*$^{-/-}$ mice 10 days after stroke. CTGF, connective tissue growth factor; IGFBP7, insulin-like growth factor binding protein-7; IL-8, interleukin-8; osteo, osteoprotegerin. Values are mean ± SD. Unpaired, 2-tailed Student *t* test. n = 3 per group, $^{*}P < .05$. (B) Quantitative PCR was used in freshly isolated brain microvessels to evaluate the expression of Ang-2 and Gal-3 in WT and *Vwf*$^{-/-}$ mice 10 days after stroke. Values are mean ± SD. Unpaired 2-tailed Student *t* test. n = 3 per group, $^{*}P < .05$. (C-F) Quantification of percent area occupied by vascular structures, perfused capillary length, PDGFR-β^{+} pericyte coverage, and the PS product of FITC-dextran in *Adamts13*$^{-/-}$ mice treated with control (Ad-Con) or Ang-2 adenoviruses (Ad-Ang-2), and Ad-Ang-2 in combination with dimethyl sulfoxide (DMSO) or the VEGFR-2 antagonist Su1498. Values are mean ± SD. One-way ANOVA followed by Bonferroni multiple comparison test. n = 6 per group, $^{*}P < .05$. (G-J) Quantification of percent area occupied by vascular structures, perfused capillary length, PDGFR-β^{+} pericyte coverage, and the PS product of FITC-dextran in *Adamts13*$^{-/-}$ mice treated with saline or rGal-3, rGal-3 in combination with DMSO or the VEGFR-2 antagonist Su1498. Values are mean ± SD. One-way ANOVA followed by Bonferroni multiple comparison test. n = 6 per group, $^{*}P < .05$. (K) (Left) Immunoblots of VEGFR-2 and phosphorylated VEGFR-2 in brain microvessels of WT mice, *Adamts13*$^{-/-}$ mice, *Adamts13*$^{-/-}$ mice treated with Ad-Con or Ad-Ang-2, *Adamts13*$^{-/-}$ mice treated with saline or rGal-3, *Vwf*$^{-/-}$ mice, and WT mice treated with vehicle or rADAMTS13. (Right) Quantitative determination of phosphorylated VEGFR-2 in brain microvessels for each group. Values are mean ± SD. n = 5 per group. $^{*}P < .05$, One-way ANOVA followed by Bonferroni multiple comparison test. $^{\#}P < .05$, Unpaired, 2-tailed Student *t* test. (L) ADAMTS13 regulates angiogenesis and vascular remodeling by targeting VWF. ADMATS13 deficiency results in enhanced plasma UL-VWF and suppressed Ang-2/Gal-3–pVEGFR-2 signaling and as a consequence impaired vascular remodeling and functional recovery.

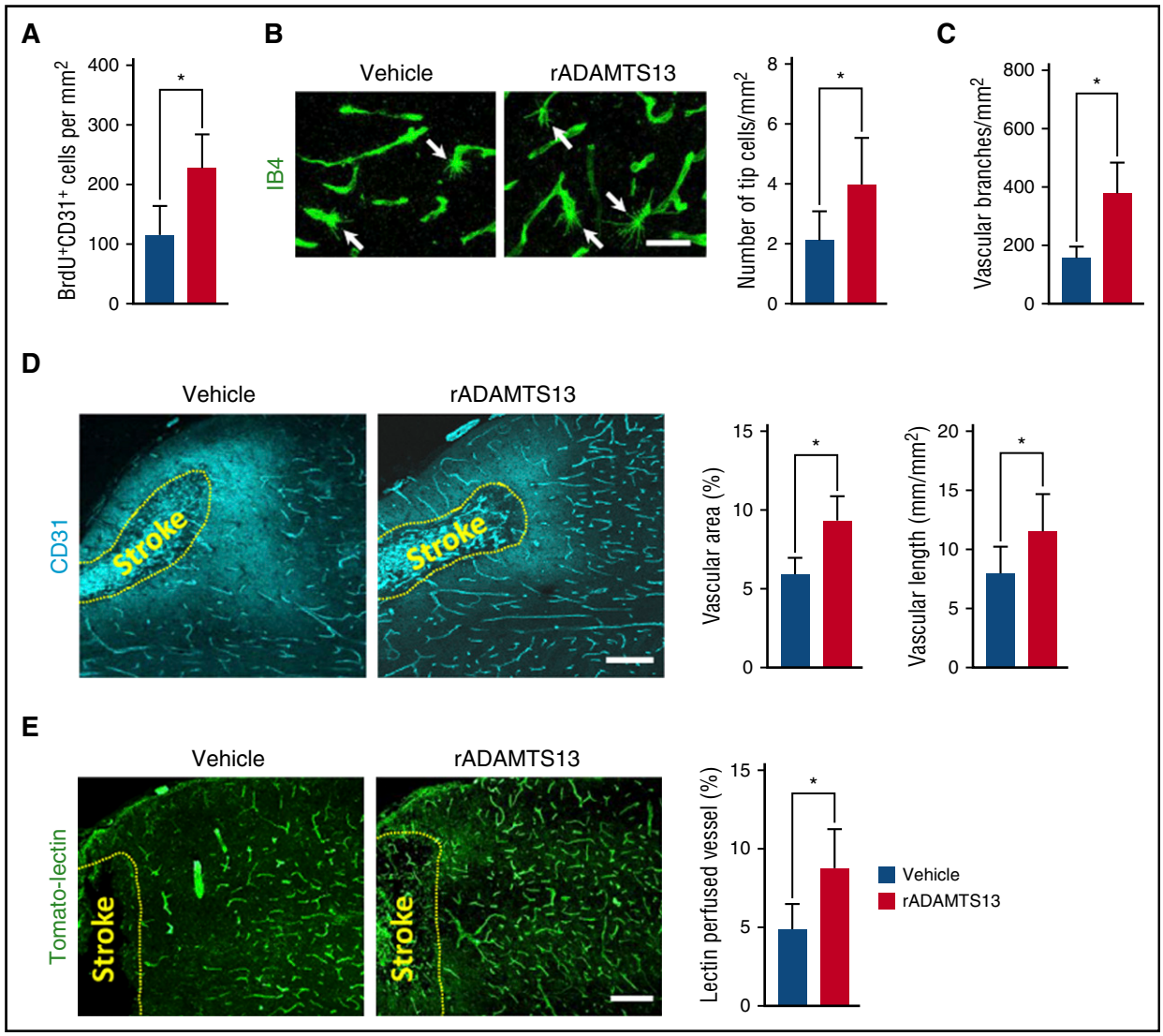

Figure 5. rADAMTS13 enhances neovascularization during stroke recovery. (A) Quantification of BrdU$^+$/CD31$^+$ endothelial cells in WT mice treated with vehicle or rADAMTS13 at 14 days after stroke. (B) Representative images and quantification of IB4$^+$ endothelial tip cells in WT mice treated with vehicle or rADAMTS13. Bar = 25 μm. (C) Quantification of vascular branches in WT mice treated with vehicle or rADAMTS13. (D) Representative images of CD31$^+$ microvessels in WT mice treated with vehicle or rADAMTS13, and quantification of CD31$^+$ microvascular length and percent area occupied by vascular structures for each group. Scale bar = 100 μm. (E) Representative images of tomato-lectin–perfused vessels and quantification of lectin-perfused vessel area in WT mice treated with vehicle or rADAMTS13. Scale bar = 200 μm. Values are mean ± SD. Unpaired, 2-tailed Student *t* test. n = 6 per group, $^*P < .05$.

Thus, we next investigated whether extra administration of exogenous rADAMTS13 into WT mice could improve vascular remodeling. Compared with vehicle controls, mice treated with rADAMTS13 showed twofold, 1.9-fold, and 1.5-fold increases in BrdU$^+$/CD31$^+$ endothelial cells, IB4$^+$ endothelial tip cells, and vascular branches (Figure 5A-C), respectively. Both intraventricular and intravenous administration of rADAMTS13 significantly increased the length and area of microvessels when compared with the vehicle group (Figures 5D and 6A). We also observed a marked 76% increase in lectin-perfused vessels in mice subjected to intraventricular rADAMTS13 treatment compared with mice treated with vehicle (Figure 5E). Multiphoton microscopy analysis of IV injected FITC-dextran revealed that intravenous administration of rADAMTS13 caused a significant increase in the length of perfused cortical microvessels (Figure 6B). Notably, extravascular accumulation of circulating dextran and IgG were dramatically reduced in the brains of mice treated with intraventricular rADAMTS13 (Figure 7A-B). Intravenous administration of rADAMTS13 was also similarly effective in reducing BBB permeability (Figure 6C). Next, we investigated whether the improvement of vascular remodeling by exogenous ADAMTS13 is abolished by exogenous VWF. We found that treatment with VWF in combination with rADAMTS13 significantly reduced microvessels, the length of perfused cortical microvessels, and BBB permeability compared with mice treated with rADAMTS13 alone (Figure 6A-C). Furthermore, we observed that treatment of mice with rADAMTS13 induced a significant increase in VEGFR-2 phosphorylation (Figure 4K), which is consistent with a recent in vitro study.[22] Immunohistochemical quantification indicated 44% and 64% increases in CD13$^+$ and PDGFR-β$^+$ pericyte coverage, respectively, in rADAMTS13-treated mice compared with vehicle-treated mice (Figure 7C; supplemental Figure 5B). There was also a significant 51% increase in the NG2$^+$ pericyte coverage in rADAMTS13-treated mice (supplemental Figure 5C). Consistent with these findings, collagen IV$^+$ basement membrane coverage was 41% higher, and α-SMA coverage was significantly increased on cortical

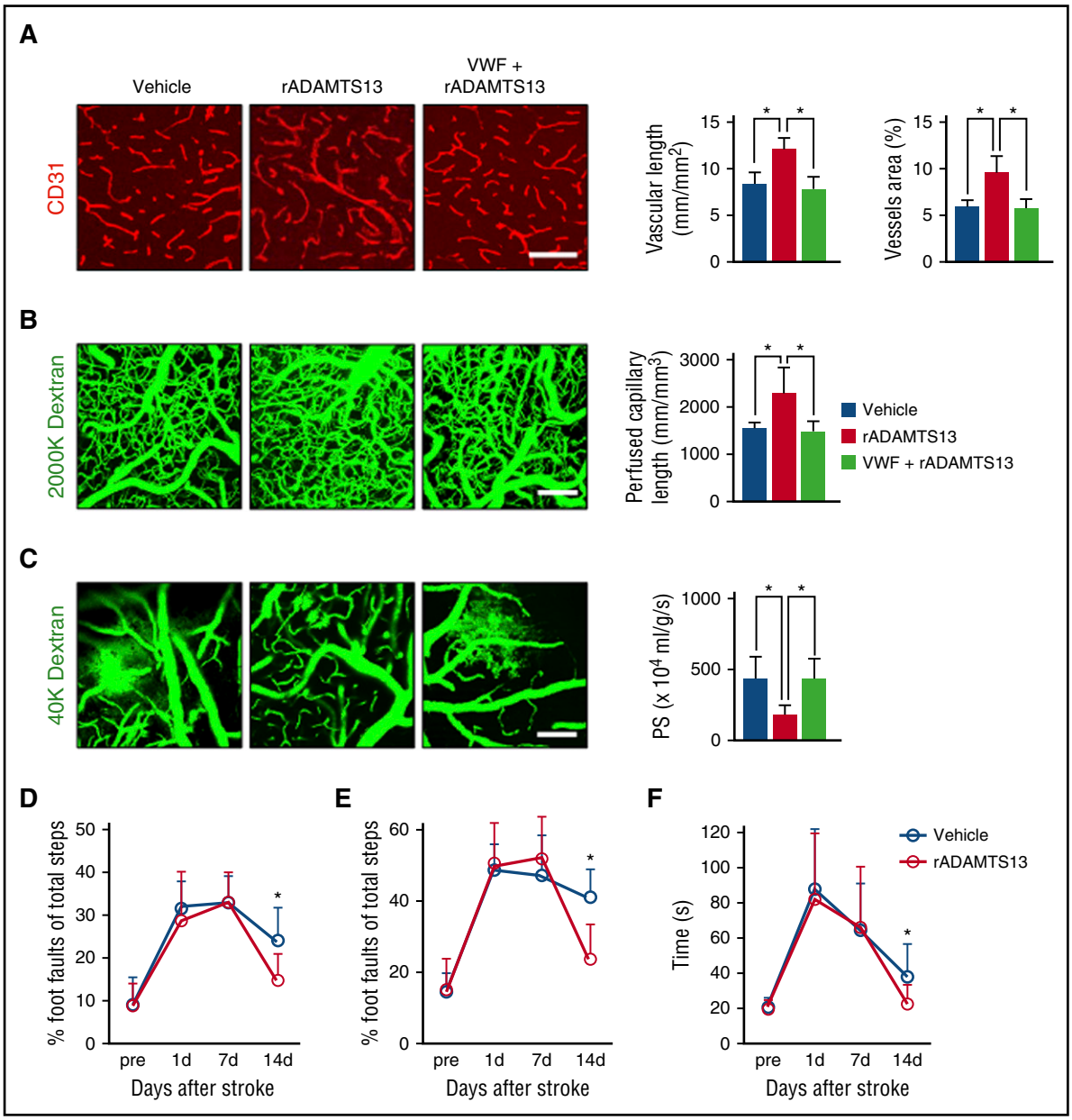

Figure 6. Intravenous administration of rADAMTS13 enhances neovascularization, promotes vascular remodeling, and improves neurological functions after stroke. (A) Representative images and quantification of CD31$^+$ microvessels in WT mice treated with intravenous vehicle rADAMTS13 or rADAMTS13 in combination with VWF at 14 days after stroke. Scale bar = 100 μm. Values are mean ± SD. One-way ANOVA followed by Bonferroni multiple comparison test. n = 6 per group, $^*P < .05$. (B) Representative in vivo multiphoton microscopic images of cortical capillaries with IV injected FITC-dextran (MW = 2 000 000 Da) and quantification of perfused capillary length in WT mice treated with intravenous vehicle rADAMTS13 or rADAMTS13 in combination with VWF at 14 days after stroke. Scale bar = 100 μm. Values are mean ± SD. One-way ANOVA followed by Bonferroni multiple comparison test. n = 6 per group, $^*P < .05$. (C) Representative in vivo multiphoton microscopic images of IV injected FITC-dextran (MW = 40 000 Da) leakage from cortical vessels and quantification of the PS product of FITC-dextran in WT mice treated with intravenous vehicle rADAMTS13 or rADAMTS13 in combination with VWF at 14 days after stroke. Scale bar = 100 μm. Values are mean ± SD. One-way ANOVA followed by Bonferroni multiple comparison test. n = 6 per group, $^*P < .05$. (D-F) Beam-walking and tape removal tests in WT mice treated with intravenous vehicle or rADAMTS13. Mice were subjected to stroke and treated with vehicle or rADAMTS13 on day 7. Values are mean ± SD. Unpaired, 2-tailed Student *t* test. n = 8 per group, $^*P < .05$.

capillaries of rADAMTS13-treated mice (Figure 7D; supplemental Figure 5D). To test whether the improved vascular function were associated with behavioral outcome, we next compared the performance of mice in the beam-walking test and adhesive tape removal test. At 1 to 7 days after stroke, no significant differences in behavioral deficits were detected in rADAMTS13-treated mice compared with vehicle-treated mice. However, both intraventricular and intravenous administration of rADAMTS13 improved neurological functions at 14 days (Figures 6D-F and 7E-G).

Discussion

In this study, we showed that deficiency of ADAMTS13 resulted in reduced neovascularization, increased loss of cerebrovascular integrity, and amplified vascular damage in the peri-infarct cortex in mice subjected to stroke. Treatment with rADAMTS13 beginning 7 days after stroke significantly enhanced neovascularization, restored impaired vascular function, and improved neurological functions at 14 days. Moreover, we demonstrated that ADAMTS13 promoted

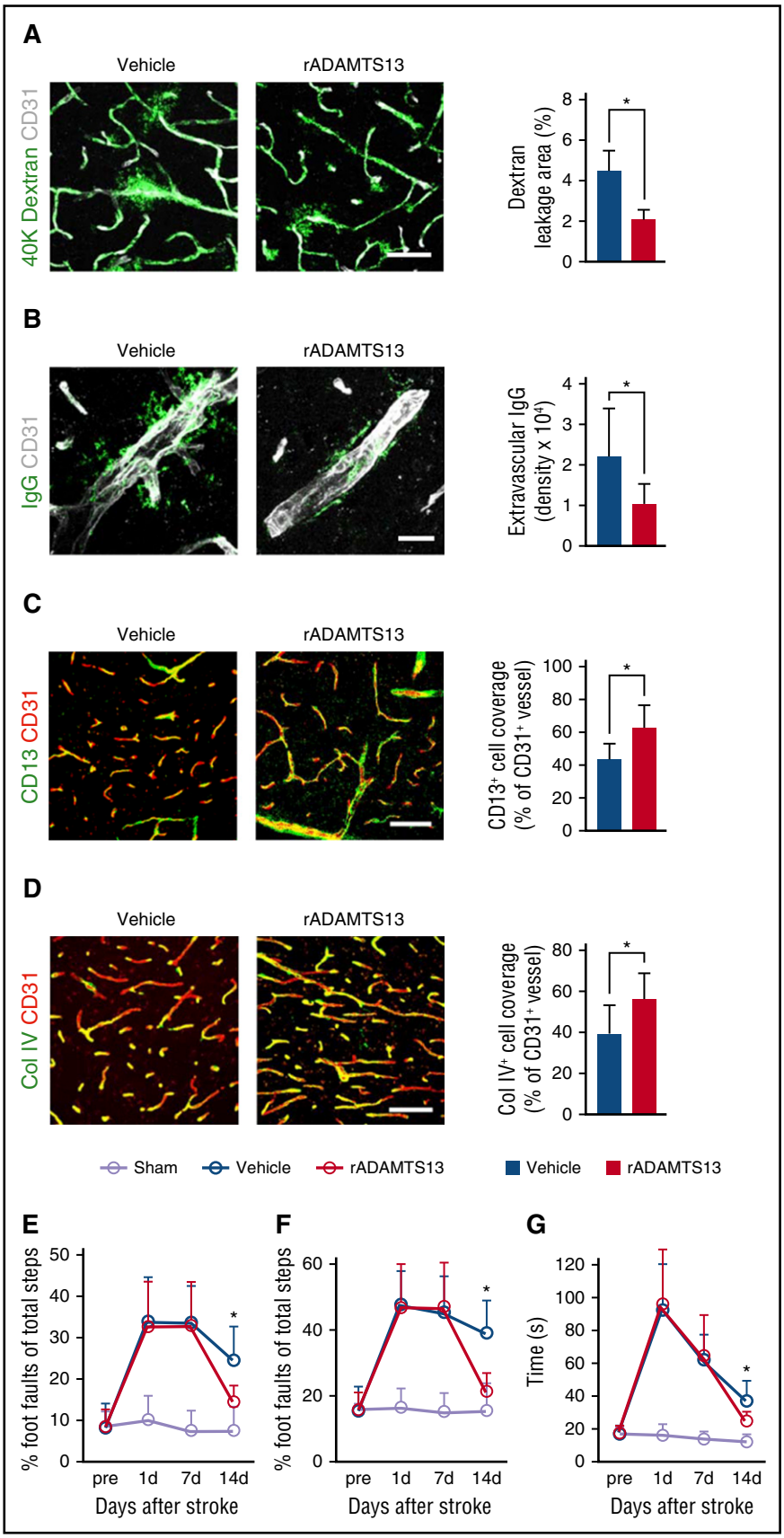

Figure 7. Reduced vascular damage and improved stroke outcomes in rADAMTS13- treated mice. (A) (Left) At 14 days after stroke, mice were given an intravascular injection of 40 000 Da FITC-labeled dextran, and brain sections were stained with CD31. (Right) Quantification of extravascular dextran fluorescence in WT mice treated with vehicle or rADAMTS13. Scale bar = 20 μm. Values are mean ± SD. Unpaired, 2-tailed Student *t* test. n = 6 per group, $^*P < .05$. (B) Representative images of IgG deposits and CD31$^+$ microvessels in WT mice treated with vehicle or rADAMTS13 at 14 days after stroke, and quantification of extravascular IgG deposits for each group. Scale bar = 20 μm. Values are mean ± SD. Unpaired, 2-tailed Student *t* test. n = 6 per group, $^*P < .05$. (C) Representative images and quantification of CD13$^+$ pericyte coverage on CD31$^+$ microvessels in WT mice treated with vehicle or rADAMTS13. Scale bar = 50 μm. Values are mean ± SD. Unpaired, 2-tailed Student *t* test. n = 6 per group, $^*P < .05$. (D) Representative images and quantification of Col IV basement membrane coverage on CD31$^+$ microvessels in WT mice treated with vehicle or rADAMTS13. Scale bar = 50 μm. Values are mean ± SD. Unpaired, 2-tailed Student *t* test. n = 6 per group, $^*P < .05$. Effects of rADAMTS13 on forelimb (E) and hind limb (F) foot faults. Mice were subjected to stroke and treated with rADAMTS or vehicle on day 7. Values are mean ± SD. One-way ANOVA followed by Bonferroni multiple comparison test. n = 7-8 per group, $^*P < .05$. (G) Effects of rADAMTS13 on adhesive tape removal test. Values are mean ± SD. One-way ANOVA followed by Bonferroni multiple comparison test. n = 7-8 per group, $^*P < .05$.

vascular remodeling after stroke via regulation of VWF-Ang-2/Gal-3-pVEGFR-2 in brain microvessels.

Angiogenesis and vascular remodeling are essential for ischemic brain repair. In patients with stroke, there was a significant correlation between the microvessel density in the brain and delayed mortality.[7,44] In the adult brain, neovascularization is a complex and finely regulated process that consists of the sprouting of new blood vessels from preexisting vascular structures and proliferation of cerebral endothelial cells.[6,45] Here, we found that ADAMTS13 is an important regulator of new vessels formation in the peri-infarct cortex during the delayed stages after stroke. Our data showed that, by exerting inhibitory effects on the vessel sprouting and the endothelial cell replication, ADAMTS13 deficiency could restrict formation of new blood vessels. The substantial attenuation of functional revascularization in *Adamts13*$^{-/-}$ mice, as demonstrated by the reduced perfused vessels in the peri-infarct cortex, may also attributable to ADAMTS13 deficiency-mediated loss of newly formed brain vessels. Recent studies have suggested that ADMATS13 deficiency resulted in increased thrombus formation, myocardial infarction, atherosclerosis, cerebral infarction, and inflammatory responses,[11,12,46-48] whereas VWF deficiency was protective. In agreement with these findings, we found that ADAMTS 13 and VWF had opposite effects on blood vessel formation after stroke. Our findings led to the hypothesis that, by cleaving UL-VWF into less active VWF fragments, ADAMTS 13 reduces VWF-mediated vascular effects. In the present study, 8- to 10-week-old adult mice were used. However, because stroke in humans predominantly occurs in the aging population,[49] stroke models using older animals may be clinically more relevant than stroke models in young adults. To avoid the interference of female sex steroid hormones,[50] we used male mice; however, caution should be taken in extrapolating the results to stroke patients in women.

The breakdown of BBB in ischemic stroke can persist for several weeks after the ischemic insult.[30,31] Pericytes and smooth muscle cells play important roles in regulating angiogenesis and BBB leakage.[34,51-53] We found that ADAMTS13 deficiency in mice increased the ischemic damage to smooth muscle cells and pericytes, resulting in reduced pericyte and smooth muscle cell coverage on microvessels during the later phase of stroke. These effects were accompanied by reduced expression of the BBB tight junction and basement membrane proteins. We then observed amplified BBB damage in the peri-infarct cortex of *Adamts13*$^{-/-}$ mice, including significantly greater extravasation of IV administered FITC-dextran and increased extravascular accumulation of serum IgG. Preservation of the BBB is critical for maintaining the cerebral microenvironment.[54] Moreover, considering that chronic BBB breakdown is associated with microvascular reductions,[33,55] these findings may suggest that ADAMTS13 deficiency blunted new vessel growth and maturation by increasing vascular permeability.

Our data indicate that VWF is required for ADAMTS13-mediated postischemic neovascularization and BBB integrity. VWF deficiency or inhibition of VWF function with anti-VWF antibody in *Adamts13*$^{-/-}$ mice was sufficient to restore cerebrovascular defects and prevent complete loss of microvessels. This findings are in agreement with previous studies showing that VWF-deficient mice had increased angiogenesis and a higher density of blood vessels.[18] The present findings also suggest that the mechanism of action of ADAMTS13 involves Ang-2– and Gal-3–mediated VEGFR-2 activation (Figure 4L); however, other angiogenic signals may also contribute during stroke recovery.

Both VWF and Ang-2 are stored in WBPs of endothelial cells.[16,17] A recent study reported that mice deficient in VWF exhibited increased Ang-2 levels in the heart.[56] Our results confirmed these reports and showed a significant increase in Ang-2 levels in the brains of *Vwf*$^{-/-}$ mice and a significant reduction in Ang-2 expression in *Adamts13*$^{-/-}$ mice. Because of the lack of UL-VWF clearance (Figure 3A) and increased plasma VWF in *Adamts13*$^{-/-}$ mice,[11] it is interesting to speculate that decreased Ang-2 expression in these mice was caused by lack of Ang-2 secretion. Ang-2 is known to induce pericyte loss and destabilize blood vessels[57,58]; however, the role of Ang2 in vascular integrity and permeability remains controversial. Previous work suggests that Ang-2 reduced BBB permeability after stroke[59] and induced vessel stabilization in glioma,[60] and that mice deficient in Ang-2 exhibited defects in pericyte in lymphatic vessels.[61] Here we observed that overexpression of Ang-2 in Adamts13$^{-/-}$ mice increased pericyte coverage and reduced vascular damage; these apparent differences might be due to the different models used in the various studies. We also observed that VWF deficiency resulted in an increase in Gal-3 levels. Previous work has shown that Gal-3 can interact with VWF and appears to circulate in complex with VWF.[19] These results, together with our findings, raise the possibility that the decreased Gal-3 levels observed in *Adamts13*$^{-/-}$ mice was caused by VWF, most likely the UL-VWF in the circulation. Finally, we found that administration of exogenous rADAMTS13 had a beneficial effect on vascular regeneration and long-term functional outcome, further demonstrating that ADAMTS13 is a key player in the late stages of stroke. In conclusion, the present results demonstrate a new role for ADAMTS13 in pathological and therapeutic angiogenesis.

Acknowledgments

This work was supported by grants from the National Natural Science Foundation of China (Key Program 81530034, General Program 81671156 and 81471331), the National Key Research and Development Program of China, Ministry of Science and Technology of China (2016YFC1300500-501), and the Natural Science Foundation of Shanghai (14ZR1401800).

Authorship

Contribution: H.X., Y.C., and X.Y. performed experiments and analyzed and interpreted data; P.C., L.K., X.Z., H.L., L.L., L.W., X.B., and Y.Z. performed experiments; and H.X., Y.C., B.-Q.Z., and W.F. designed the study and wrote the manuscript.

Conflict-of-interest disclosure: The authors declare no competing financial interests.

Correspondence: Wenying Fan, State Key Laboratory of Medical Neurobiology, Fudan University, 138 Yixueyuan Rd, Shanghai 200032, China; e-mail: wenyingf@fudan.edu.cn.

References

1. Lo EH. Degeneration and repair in central nervous system disease. *Nat Med*. 2010;16(11):1205-1209.
2. Carmichael ST. Emergent properties of neural repair: elemental biology to therapeutic concepts. *Ann Neurol*. 2016;79(6):895-906.
3. Parr AM, Tator CH, Keating A. Bone marrow-derived mesenchymal stromal cells for the repair of central nervous system injury. *Bone Marrow Transplant*. 2007;40(7):609-619.
4. Thiyagarajan M, Fernández JA, Lane SM, Griffin JH, Zlokovic BV. Activated protein C promotes neovascularization and neurogenesis in postischemic brain via protease-activated receptor 1. *J Neurosci*. 2008;28(48):12788-12797.
5. Zhao BQ, Wang S, Kim HY, et al. Role of matrix metalloproteinases in delayed cortical responses after stroke. *Nat Med*. 2006;12(4):441-445.

6. Zhang ZG, Chopp M. Neurorestorative therapies for stroke: underlying mechanisms and translation to the clinic. *Lancet Neurol*. 2009;8(5):491-500.
7. Krupinski J, Kaluza J, Kumar P, Kumar S, Wang JM. Role of angiogenesis in patients with cerebral ischemic stroke. *Stroke*. 1994;25(9):1794-1798.
8. Sadler JE. Von Willebrand factor, ADAMTS13, and thrombotic thrombocytopenic purpura. *Blood*. 2008;112(1):11-18.
9. Zheng XL. ADAMTS13 and von Willebrand factor in thrombotic thrombocytopenic purpura. *Annu Rev Med*. 2015;66:211-225.
10. Crawley JT, de Groot R, Xiang Y, Luken BM, Lane DA. Unraveling the scissile bond: how ADAMTS13 recognizes and cleaves von Willebrand factor. *Blood*. 2011;118(12): 3212-3221.
11. Chauhan AK, Kisucka J, Brill A, Walsh MT, Scheiflinger F, Wagner DD. ADAMTS13: a new link between thrombosis and inflammation. *J Exp Med*. 2008;205(9):2065-2074.
12. Zhao BQ, Chauhan AK, Canault M, et al. von Willebrand factor-cleaving protease ADAMTS13 reduces ischemic brain injury in experimental stroke. *Blood*. 2009;114(15):3329-3334.
13. Cai P, Luo H, Xu H, et al. Recombinant ADAMTS 13 attenuates brain injury after intracerebral hemorrhage. *Stroke*. 2015;46(9):2647-2653.
14. Yancopoulos GD, Klagsbrun M, Folkman J. Vasculogenesis, angiogenesis, and growth factors: ephrins enter the fray at the border. *Cell*. 1998;93(5):661-664.
15. Eklund L, Saharinen P. Angiopoietin signaling in the vasculature. *Exp Cell Res*. 2013;319(9): 1271-1280.
16. Wagner DD, Saffaripour S, Bonfanti R, et al. Induction of specific storage organelles by von Willebrand factor propolypeptide. *Cell*. 1991; 64(2):403-413.
17. Metcalf DJ, Nightingale TD, Zenner HL, Lui-Roberts WW, Cutler DF. Formation and function of Weibel-Palade bodies. *J Cell Sci*. 2008;121(Pt 1):19-27.
18. Starke RD, Ferraro F, Paschalaki KE, et al. Endothelial von Willebrand factor regulates angiogenesis. *Blood*. 2011;117(3):1071-1080.
19. Saint-Lu N, Oortwijn BD, Pegon JN, et al. Identification of galectin-1 and galectin-3 as novel partners for von Willebrand factor. *Arterioscler Thromb Vasc Biol*. 2012;32(4):894-901.
20. Markowska AI, Jefferies KC, Panjwani N. Galectin-3 protein modulates cell surface expression and activation of vascular endothelial growth factor receptor 2 in human endothelial cells. *J Biol Chem*. 2011;286(34):29913-29921.
21. Scheppke L, Murphy EA, Zarpellon A, et al. Notch promotes vascular maturation by inducing integrin-mediated smooth muscle cell adhesion to the endothelial basement membrane. *Blood*. 2012;119(9):2149-2158.
22. Lee M, Keener J, Xiao J, Long Zheng X, Rodgers GM. ADAMTS13 and its variants promote angiogenesis via upregulation of VEGF and VEGFR2. *Cell Mol Life Sci*. 2015;72(2):349-356.
23. Fan W, Dai Y, Xu H, et al. Caspase-3 modulates regenerative response after stroke. *Stem Cells*. 2014;32(2):473-486.
24. Wang L, Fan W, Cai P, et al. Recombinant ADAMTS13 reduces tissue plasminogen activator-induced hemorrhage after stroke in mice. *Ann Neurol*. 2013;73(2):189-198.
25. Zhu X, Cao Y, Wei L, et al. von Willebrand factor contributes to poor outcome in a mouse model of intracerebral haemorrhage. *Sci Rep*. 2016;6: 35901.
26. Lenting PJ, Westein E, Terraube V, et al. An experimental model to study the in vivo survival of von Willebrand factor. Basic aspects and application to the R1205H mutation. *J Biol Chem*. 2004;279(13):12102-12109.
27. Rastegarlari G, Pegon JN, Casari C, et al. Macrophage LRP1 contributes to the clearance of von Willebrand factor. *Blood*. 2012;119(9): 2126-2134.
28. Fan YY, Hu WW, Dai HB, et al. Activation of the central histaminergic system is involved in hypoxia-induced stroke tolerance in adult mice. *J Cereb Blood Flow Metab*. 2011;31(1):305-314.
29. Chen C, Duckworth CA, Zhao Q, Pritchard DM, Rhodes JM, Yu LG. Increased circulation of galectin-3 in cancer induces secretion of metastasis-promoting cytokines from blood vascular endothelium. *Clin Cancer Res*. 2013; 19(7):1693-1704.
30. Yang Y, Thompson JF, Taheri S, et al. Early inhibition of MMP activity in ischemic rat brain promotes expression of tight junction proteins and angiogenesis during recovery. *J Cereb Blood Flow Metab*. 2013;33(7):1104-1114.
31. Yu SW, Friedman B, Cheng Q, Lyden PD. Stroke-evoked angiogenesis results in a transient population of microvessels. *J Cereb Blood Flow Metab*. 2007;27(4):755-763.
32. Bell RD, Winkler EA, Sagare AP, et al. Pericytes control key neurovascular functions and neuronal phenotype in the adult brain and during brain aging. *Neuron*. 2010;68(3):409-427.
33. Bell RD, Winkler EA, Singh I, et al. Apolipoprotein E controls cerebrovascular integrity via cyclophilin A. *Nature*. 2012;485(7399):512-516.
34. Armulik A, Genové G, Mäe M, et al. Pericytes regulate the blood-brain barrier. *Nature*. 2010; 468(7323):557-561.
35. Breslin JW, Zhang XE, Worthylake RA, Souza-Smith FM. Involvement of local lamellipodia in endothelial barrier function. *PLoS One*. 2015; 10(2):e0117970.
36. Gandhi C, Khan MM, Lentz SR, Chauhan AK. ADAMTS13 reduces vascular inflammation and the development of early atherosclerosis in mice. *Blood*. 2012;119(10):2385-2391.
37. Lenting PJ, Casari C, Christophe OD, Denis CV. von Willebrand factor: the old, the new and the unknown. *J Thromb Haemost*. 2012;10(12): 2428-2437.
38. Daly C, Eichten A, Castanaro C, et al. Angiopoietin-2 functions as a Tie2 agonist in tumor models, where it limits the effects of VEGF inhibition. *Cancer Res*. 2013;73(1):108-118.
39. Thomas M, Augustin HG. The role of the angiopoietins in vascular morphogenesis. *Angiogenesis*. 2009;12(2):125-137.
40. Nangia-Makker P, Honjo Y, Sarvis R, et al. Galectin-3 induces endothelial cell morphogenesis and angiogenesis. *Am J Pathol*. 2000;156(3):899-909.
41. Young CC, Al-Dalahmah O, Lewis NJ, et al. Blocked angiogenesis in Galectin-3 null mice does not alter cellular and behavioral recovery after middle cerebral artery occlusion stroke. *Neurobiol Dis*. 2014;63:155-164.
42. Horie N, Pereira MP, Niizuma K, et al. Transplanted stem cell-secreted vascular endothelial growth factor effects poststroke recovery, inflammation, and vascular repair. *Stem Cells*. 2011;29(2):274-285.
43. Maliba R, Lapointe S, Neagoe PE, Brkovic A, Sirois MG. Angiopoietins-1 and -2 are both capable of mediating endothelial PAF synthesis: intracellular signalling pathways. *Cell Signal*. 2006;18(11):1947-1957.
44. Krupinski J, Kaluza J, Kumar P, Wang M, Kumar S. Prognostic value of blood vessel density in ischaemic stroke. *Lancet*. 1993;342(8873):742.
45. Asahara T, Murohara T, Sullivan A, et al. Isolation of putative progenitor endothelial cells for angiogenesis. *Science*. 1997;275(5302):964-967.
46. Chauhan AK, Motto DG, Lamb CB, et al. Systemic antithrombotic effects of ADAMTS13. *J Exp Med*. 2006;203(3):767-776.
47. Gandhi C, Motto DG, Jensen M, Lentz SR, Chauhan AK. ADAMTS13 deficiency exacerbates VWF-dependent acute myocardial ischemia/ reperfusion injury in mice. *Blood*. 2012;120(26): 5224-5230.
48. Gandhi C, Ahmad A, Wilson KM, Chauhan AK. ADAMTS13 modulates atherosclerotic plaque progression in mice via a VWF-dependent mechanism. *J Thromb Haemost*. 2014;12(2): 255-260.
49. Ramirez-Lassepas M. Stroke and the aging of the brain and the arteries. *Geriatrics*. 1998; 53(Suppl 1):S44-S48.
50. Hurn PD, Vannucci SJ, Hagberg H. Adult or perinatal brain injury: does sex matter? *Stroke*. 2005;36(2):193-195.
51. Armulik A, Abramsson A, Betsholtz C. Endothelial/pericyte interactions. *Circ Res*. 2005;97(6):512-523.
52. Hall CN, Reynell C, Gesslein B, et al. Capillary pericytes regulate cerebral blood flow in health and disease. *Nature*. 2014;508(7494):55-60.
53. Simons M, Eichmann A. Molecular controls of arterial morphogenesis. *Circ Res*. 2015;116(10): 1712-1724.
54. Zlokovic BV. The blood-brain barrier in health and chronic neurodegenerative disorders. *Neuron*. 2008;57(2):178-201.
55. Paul J, Strickland S, Melchor JP. Fibrin deposition accelerates neurovascular damage and neuroinflammation in mouse models of Alzheimer's disease. *J Exp Med*. 2007;204(8): 1999-2008.
56. Yuan L, Chan GC, Beeler D, et al. A role of stochastic phenotype switching in generating mosaic endothelial cell heterogeneity. *Nat Commun*. 2016;7:10160.
57. Ziegler T, Horstkotte J, Schwab C, et al. Angiopoietin 2 mediates microvascular and hemodynamic alterations in sepsis. *J Clin Invest*. 2013;123(8):3436-3445.
58. Augustin HG, Koh GY, Thurston G, Alitalo K. Control of vascular morphogenesis and homeostasis through the angiopoietin-Tie system. *Nat Rev Mol Cell Biol*. 2009;10(3):165-177.
59. Marteau L, Valable S, Divoux D, et al. Angiopoietin-2 is vasoprotective in the acute phase of cerebral ischemia. *J Cereb Blood Flow Metab*. 2013;33(3):389-395.
60. Valable S, Eddi D, Constans JM, et al. MRI assessment of hemodynamic effects of angiopoietin-2 overexpression in a brain tumor model. *Neuro-oncol*. 2009;11(5):488-502.
61. Shimoda H, Bernas MJ, Witte MH, Gale NW, Yancopoulos GD, Kato S. Abnormal recruitment of periendothelial cells to lymphatic capillaries in digestive organs of angiopoietin-2-deficient mice. *Cell Tissue Res*. 2007;328(2):329-337.